"Physics of Auroral Phenomena", Proc. XXVIII Annual Seminar, Apatity, pp. 74-77 , 2005
© Kola Science Center, Russian Academy of Science, 2005

Polar
Geophysical
Institute

CURRENT SHEETS IN SPACE PLASMA

I.M. Podgorny[1], A.I. Podgorny[2]

[1]*Institute for Astronomy RAS, Moscow, Russia, podgorny@inasan.rssi.ru,*
[2]*Lebedev Physical Institute RAS, Moscow, Russia*

Abstract. The important features of a current sheet (CS) are plasma flow along the sheet and the normal magnetic field component. On the basis of numerical experiments, space measurements and laboratory experiments it is possible to make conclusions about CS generation and its decay, including the role of magnetic field reconnection. The differences in the behavior of the CS of the Earth, planets, Sun and interplanetary space are considered

Introduction

CSs are widely spread objects in space plasma. They exist in the interplanetary space, in the tails of the Earth and other planet magnetospheres, in the tails of comets, and in the solar corona. The CS magnetic field is responsible for energy storage that releases during solar flares and substorms. The important features of CS are plasma flow along the sheet and the normal magnetic field component. There are two strong arguments against a possibility of a neutral CS (zero normal magnetic component) existence:

1. Numerous theoretical works show that a neutral CS is very unstable.
2. It is impossible to propose any mechanism of a neutral CS formation in the laboratory, space or in numerical simulation.

The CS attracts attention because the magnetic field energy accumulated in the magnetic field $\int(B^2/8\pi)dv$ can dissipate, accompanied by plasma heating. Effective plasma heating is possible only in low β plasma. On the basis of numerical experiments, space measurements and laboratory experiments it is possible to conclude about CS generation and dissipation, including the role of magnetic field reconnection. Reconnection can occur in the vicinity of a neutral line (line B=0) of X-type, where oppositely directed magnetic lines can merge. As a result, plasma flows into the CS. Within MHD consideration, plasma flows together with frozen-in magnetic lines. Two oppositely directed magnetic lines can approach each other and merge producing two new magnetic lines inside the CS. As a result, new topology class of magnetic lines appears inside the CS. The energy flux $\frac{B^2}{8\pi} SV_{in}$ in the CS is determined by the Poynting vector. Such a reconnection model requires the magnetic lines to be frozen in plasma inflow into the CS and plasma (with magnetic lines) outflow from the X-line in the opposite directions along the CS (Fig. 1). The rate of magnetic reconnection in a long CS has been considered by Parker and Sweet for non-compressible plasma, without taking into account plasma acceleration along the sheet by the $\mathbf{j}\times\mathbf{B}/c$ force. They assumed that everywhere except X-line vicinity the magnetic field lines are frozen into the plasma ($V\times B/c >> j/\sigma$) and used the continuity equation in the form of divV=0. At such a condition, the magnetic reconnection rate $V_{in}=V_A Re_m^{-1/2}$ is rather slow (here V_{in} is the plasma inflow velocity called the reconnection rate, V_A is the Alfven velocity, and Re_m is the magnetic Reynolds number}. A higher reconnection rate takes place in a compressible plasma, with taking into account the $\mathbf{j}\times\mathbf{B}/c$ force inside the CS: $V_{in}=V_A(B_n/B_0)^{1/3}(Re_m\beta)^{-1/3}$. Here, $Re_m=4\pi\sigma V_A L/c^2$, L is the CS length, σ is the conductivity, B_0 is the CS magnetic field, B_n is the normal magnetic component, and $\beta=4\pi nkT/B_0^2$. But even this value of V_{in} can not explain the explosive energy release during solar flares or substorms. For explosive energy release, a transition of the CS into unstable state is needed, followed by its fast decay [1].

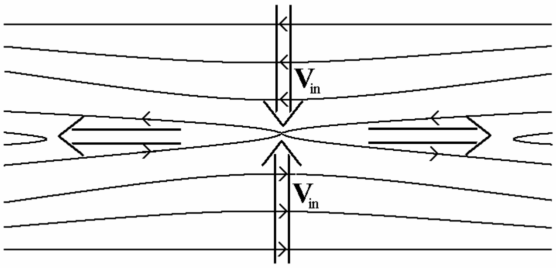

Fig. 1.

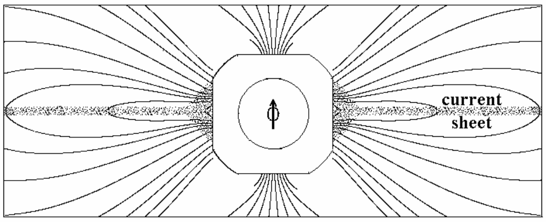

Fig.2.

Interplanetary current sheet

Interplanetary CS generation takes place at solar wind thermal expansion in the global solar magnetic field [2]. This phenomenon was numerically simulated in the dipole magnetic field corresponding to solar minimum activity (Fig. 2). A ring CS appears due to corona thermal expansion. Current generation takes place inside the heliospheric CS due to the Lorenz electric field. In the case of the ring current, the Ohm law can be written as $\mathbf{j}=-\sigma\,\mathbf{V}\times\mathbf{B}/c$. So, the normal magnetic field component and the plasma velocity directed from the Sun are necessary for heliospheric CS formation. The heliospheric CS is not a neutral one, as has often been claimed.

CS plasma motion to the Sun is impossible in heliospheric CS because the reverse velocity should change current direction. As a result, the formation of the reconnection pattern in the heliospheric CS (Fig. 1) is impossible. An occasionally formed X-line can not provide reconnection because in such a case it would have to move from the Sun with the velocity exceeding that of the solar wind. There is no cause for providing such X-line motion.

Comet current sheet

The current generation in planetary and comet magnetospheres takes place in the boundary layers due to solar wind flow across the magnetic field and Lorenz electric field $\mathbf{E} = -\mathbf{V}\times\mathbf{B}/c$ production. This current is closed inside the CS. The $\mathbf{j}\times\mathbf{B}/c$ force inside the CS determines the plasma flow along the sheet. This force is always directed from the comet nucleus. The comet magnetosphere with a tail CS forms at magnetized solar wind plasma interaction with plasma that is produced by ionization of the gas evaporated from the icy nucleus of a comet [3]. The ionization is due to solar radiation. The magnetic field lines, piled up around the nucleus surrounded by comet plasma, are stretched in the anti-solar direction. The $\mathbf{j}\times\mathbf{B}/c$ force stretches the comet plasma, producing a long luminous tail. Plasma in the tail always moves away from the nucleus. For the reconnection of tail lines to occur, the plasma has to move toward the nucleus, but such a flow is impossible, because comet plasma is created at evaporation of nucleus. The velocity pattern for reconnection, shown in Fig 1 can not form in the tail. The comet tail disruption is observed at crossing the heliospheric CS. It is produced due to reconnection on the subsolar neutral line (Fig. 3). Such a reconnection occurs because the direction of interplanetary field becomes opposite to the comet magnetic field in the subsolar region [4]. The induced comet magnetic field vanishes, and the comet tail tears off. After that, the magnetic lines of opposite direction pile up, and a new induced magnetosphere with a new tail form.

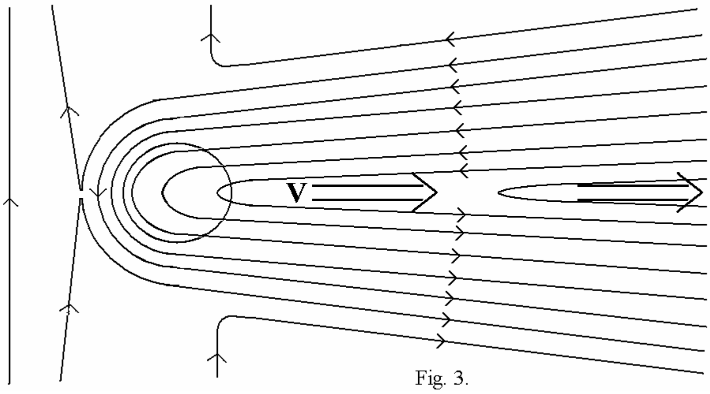

Fig. 3.

Current sheet in the Earth's magnetotail

The solar wind flows around the Earth's magnetosphere and stretches the magnetic field lines along the wind velocity. The mechanism of current generation in the Earth's magnetotail is similar to that existing in the comet magnetosphere. However, a velocity pattern observed during steady state conditions is different. The jB_n/c force is applied to the CS plasma, accelerating it toward the Earth. ∇p force acts in the opposite direction. In the stationary condition $jB_n/c > \nabla p$. This means that plasma enters the CS in the distant tail, then being accelerated to the Earth. Apparently, a neutral line in the Earth tail CS exists in the distant tail, where slow reconnection supplies a weak plasma flow toward the Earth. The magnetic lines and velocities (the arrows) are shown in Fig. 4a. The scheme of current generation is shown in Fig. 4b. The rate of dissipation of the energy accumulated in the tail magnetic field is determined by plasma conductivity and current sheet thickness. The time of dissipation $t \sim 4\pi\sigma\delta^2/c^2$ is of the order of 10^{13} c. Such a dissipation can not play any role. During long intervals between substorms, the tail current sheet demonstrates a very high stability, which can be provided due to the plasma velocity along the sheet and normal magnetic component.

At the beginning of substorm, a new neutral line forms at the distance of 20-30 Earth's radii (Fig. 4c). X-line formation is associated with the disturbances in the solar wind produced by a solar flare. Fast magnetic field dissipation arises due to instability because the plasma inflow into the current sheet can not compensate plasma loss due to its ejection along the sheet in both directions, and the current sheet becomes very narrow. The southward interplanetary magnetic field, once appeared, can initiate reconnection. A classical example of plasma motion in the magnetosphere in the presence of the southward IMF component is a well-known Dungey pattern.

Fields and currents in the stationary Earth's current sheet

Let us consider the fields and currents in the CS of the Earth's tail based on the Ohm law taken in the form

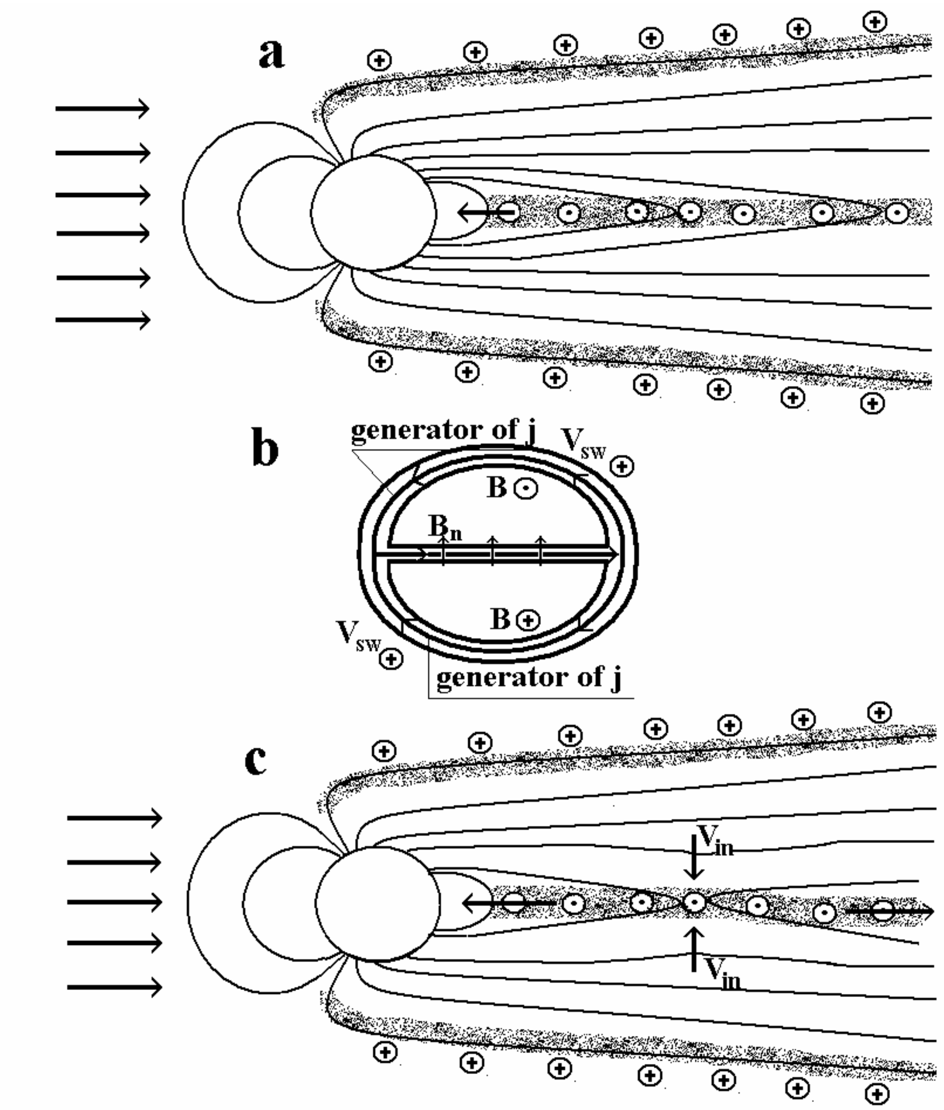

Fig. 4.

$$\frac{\mathbf{j}}{\sigma} = \mathbf{E} + \frac{1}{\mathbf{c}}\mathbf{V}\times\mathbf{B} - \frac{1}{\mathbf{nec}}\mathbf{j}\times\mathbf{B} + \frac{\nabla\mathbf{P_e}}{\mathbf{ne}} \quad (1), \qquad \text{where } \sigma = \frac{ne^2\tau_e}{m_e}.$$

In a typical CS the magnetic field is $B_x=2\times10^{-4}$G, with the normal magnetic field component being $B_n=10^{-5}$G, the plasma density in CS is n=0,5 cm^{-3}, and CS thickness is $\delta=5\times10^{8}$cm. In this case, the current density is $j=B_xc/2\pi\delta = 2\times10^{-3}$CGSE = 7×10^{-13}A/cм^2. The corresponding current velocity is ~10^7cм/c. During a substorm, the CS thickness drops, but the current density increases by an order of magnitude. Evidently, the current velocity maximum is restricted by an instability development. The current velocity and, as a result, CS thickness are determined by beam or ion sound instability.

Let us compare two last terms in eq. (1), i.e. $B_xB_n/2\pi\delta$ and $P/L=B_x^2/8\pi L$ at the pressures balance condition $nkT=B_x^2/8\pi$. The pressure gradient along the CS can be neglected if the geomagnetic tail length $L\gg\delta\, B_x/4B_n$. This always holds in the Earth's tail.

In the absence of the external electric circle that closes the Hall current, the current directed along the CS is zero ($j_x=0$). The earthward (Hall) electric field $E_x=jB_n/nec \sim 10^{-6}$V/cm exists inside the CS. At a substorm, the CS thickness drops by an order of magnitude, and the Hall potential difference can reach 10^5V over the part of the tail up to ~20 Earth radii. Such a potential difference is capable of generating field-aligned currents and accelerating electrons that produce aurora. At complete Hall current locking in the CS, the Ohm law becomes the same as for B=0, i.e. $\mathbf{j}=\sigma\mathbf{E}$.

The maximum current directed along the CS is reached at zero external resistance. In that case $E_x=0$, and the current along the X-axis is the Hall current $j_x=j_h=\omega\tau j$. Here ω is the electron cyclotron frequency, τ the electron-ion collision time $\omega\tau = 5\times10^{11}T_ev^{3/2}B/n$. In the Earth's CS $\omega\tau \sim 3\times10^{11}$, and then j_h~0.2A/cm^2. Obviously, this value of j_x is inconsistent with the space measurements. According to [5], j_x is ~10^{-13}A/cm^2. Hence, the electric field directed along the CS can not be close to zero, and j_x is strongly restricted.

The self consistent **j** value corresponds to a rather strong locking of the Hall current. In that case, a part of the current of the CS is the Hall current produced by the earthward electric field. The components of current density in geocentric coordinates can be written in the form:

$$\mathbf{j_x} = \mathbf{E_x}\frac{\sigma}{1+(\omega\tau)^2} - (\mathbf{E_y} - \mathbf{V_x B_n}/\mathbf{c})\frac{\omega\tau\sigma}{1+(\omega\tau)^2};\ldots\ldots\ldots\mathbf{j_y} = \mathbf{E_x}\frac{\omega\tau\sigma}{1+(\omega\tau)^2} + (\mathbf{E_y} - \mathbf{V_x B_n}/\mathbf{c})\frac{\sigma}{1+(\omega\tau)^2}$$

Supposing j_h=0 and excluding E_x, one gets the Ohm law as $j=\sigma(E_y-V_xB_n/c)$. For the current density $j=7\times10^{-13}$A/cm^2 and plasma velocity $V_x \sim 10^7$cm/s, the generated electric field is $E_y \sim V_xB_n \sim 10^{-6}$V/cm, with the possible maximum of the applied potential difference $\varphi \sim 20R_EE_y$ exceeding 10kV. For $V_x \sim 5\times10^7$cm/s, $\varphi \sim 50$kV. This value of the potential difference is in agreement with the measurements in the polar cap.

Solar flares

The solar flare model shown in Fig. 5 means to explain all major phenomena associated with a solar flare. The thin lines present magnetic field lines. The thick lines show the field-aligned currents with their directions. The CS above an active region appears in the vicinity of a singular magnetic line due to MHD disturbances coming from the photosphere. Plasma can flow into the CS according to the velocity pattern shown in Fig. 1. There are no reasons why this pattern could not be realized. Plasma flows into the CS with the frozen-in magnetic field, and after the reconnection is accelerated by **j**×**B**/c force. In the course of evolution, the CS transfers to an unstable state. Its decay provides magnetic energy transformation into plasma kinetic energy and particle acceleration up to relativistic energy. Plasma accelerated upward produces CME. The hot plasma moves with the contracted magnetic lines downward, producing post flare loops. The Hall electric field directed along the CS generates a system of FACs that are closed in the chromosphere. The electrons accelerated in the FACs precipitate to the solar surface. The acceleration of relativistic proton is produced by the $\mathbf{E} = -\mathbf{V}_{in}\times\mathbf{B}/\mathbf{c}$ electric field along the magnetic X-line perpendicular to the plane of Figure 5. The electric field increases during a fast reconnection. In a general case, the X-line is not a neutral one. The magnetic field along the X-line helps to stabilize proton acceleration. The estimations show that such a mechanism is capable of generating relativistic energy. Solar flare model has been described in detail in [6]

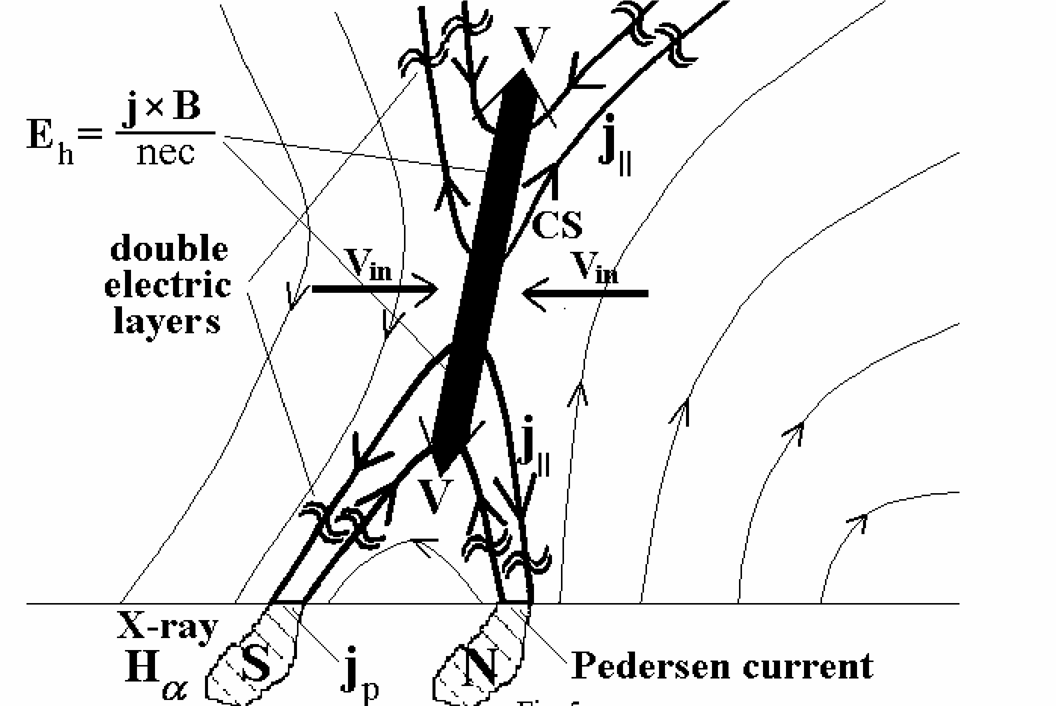

Fig. 5.

References

1. Podgorny A.I. *Plasma Phys. and Controlled Fusion.* **31**, 1271 (1989).
2. Podgorny I. M. and Podgorny A. I., Minami S., and Morimoto M. *Astronomy Report.* **79**, 475 (2004).
3. Podgorny I. M. *Adv. Space Res.* **1**, 385 (1981).
4. Podgorny I. M., Andrienko D. A., Kleshchenok V. V. and Mischishina I. I. *Astro. Letts. And Comunication.* **28**, 33 (1990).
5. Ershkovich A. I., Israelevich P. L. and Tsyganenko N. A. *JGR.* **106**, 25919 (2001).
6. Podgorny A.I. and Podgorny I. M. In *Phys. of Auroral Phenomena. Proc. 25th Annual Seminar.* 2002, p. 133.